Diffusion across a Gel-Gel Interface – Molecular-Scale Mobility of Self-Assembled 'Solid-Like' Gel Nanofibres in Multi-Component Supramolecular Organogels

Jorge Ruíz-Olles and David K. Smith*

Department of Chemistry, University of York, Heslington, York, YO10 5DD, UK

1 Materials and Methods

1.1 Materials Used. Lysine dendrons were synthesised according to previously reported methods and all data were in agreement with previous reports.[1] All other reagents were provided from standard chemical suppliers.

1.2 Instrumental Methods. Thermal stability was recorded on a Huber Ministat 230 circulator oil bath. TEM and SEM images were obtained by Meg Stark at Biology Technology Faculty, University of York, using a FEI Tecnai 12 Bio TWIN operated at 120 kV for the TEM images and a JEOL JSM-7600F operated at 3 kV for the SEM images. Atomic Force Microscopy (AFM) images were recorded using a Dimension Icon AFM from Bruker. ^{1}H NMR spectra were recorded on a Jeol ECX spectrometer (^{1}H 400 MHz), all chemical shifts (δ) are quoted to ppm and referenced to a residual solvent peak. Circular Dichroism (CD) spcroscopy was performed on a Jasco J810 circular dichromator fitted with a Peltier temperature control unit using a quartz cell with a path length of 1 mm using the following settings: Data Pitch – 0.5 nm, Scanning Mode – Continuous, Scanning Speed – 100 nm min-1, Response – 1 s, Bandwidth – 2 nm, Accumulation – 5. All CD data are presented as ellipticity and recorded in mdeg.

1.3 T_{gel} Determination. T_{gel} values were observed by reproducible tube inversion methodology. All the samples with different concentrations of heparin and heparin-C16-DAPMA aggregates that resulted in gel formation and were placed into a thermo-controlled oil bath, with an initial temperature of 25°C. The temperature was set to rise to 100 °C. At each increase of 5 °C, approximately, the tubes were removed from the bath and turned upside down. The stability of the gels was observed and the T_{gel} was considered as the temperature when the gel started to deform.

1.4 Sample Preparation for Imaging. *TEM Imaging.* A small piece of gel was taken with a spatula and was lightly rubbed against a copper grid standard. The sample was then left to evaporate for at least 30 min before introducing into the high vacuum chamber. No stain was used with any sample because of the incompatibility between aqueous and organic solvents –

for this reason contrast was reduced. *SEM Imaging.* An ambient drying method was used, involving simple drying of the gel open to the surrounding air at room temperature. The process consists of taking a small piece of gel and placing it on an aluminium stub. Samples were left to dry in the bench covered by a beaker to avoid dust particles or excessive flow of air. Samples were placed in the SEM cavity and sputtered by a thin layer of palladium prior to analysis. *AFM Imaging.* The preparation of samples was achieved by drying at ambient temperature and pressure following the same procedure as that used for SEM. Samples were covered by a glass flask to prevent moisture and dust in the sample.

1.5 Rheology Experiments. The rheological testing was performed using the Kinexus Malvern Pro Plus rheometer with a aprallel plate geometry. The variation of viscosity properties over time was monitored with the rheometer was programmed to record viscoelastic values (viscosity program). A toluene solution of dendron (10 mM) was introduced into an aluminium weighing boat in which the viscosity analysis was going to be performed. The aluminium vessel was placed in the rheometer and the probe was placed touching the solution of dendron. The rheometer was then activated and starts to record typical values of viscosity for a solution. At time = 0, we then rapidly added the solution of other component (amine, concentration = 10 mM) into the aluminium vessel. From that moment, the two components can start to interact and the viscosity should increase as the sol-gel transition progresses. The increase in viscosity over time can be analysed and typically exhibited a two step process of rapid gelation followed by ageing of the dynamic network.

1.6 Diffusion Cell Experiments. An amount of gel (5.6 mL) was prepared in 8 mL vials. Gels have a final concentration of 5 mM, which means that the solutions of the two components each have a concentration of 10 mM. To these solutions, a reference material (diphenylmethane)

was also incorporated at the desired concentration if needed. The gels in vials were heated until they completely dissolved. The diffusion cell (see Section 3) was ready to be filled with the gels, and an aluminium barrier was inserted to avoid the mixing of the two gels when loading them into the cell. Then, the gels were solidified by lowering the temperature with an ice bath in contact with the external cell walls. Once the gels were in the solid state, the aluminium separator was removed, to bring the gels into contact for the first time, creating a gel-gel interface. The cell was placed in a chamber full of toluene to maintain solvation while diffusion takes place. The diffusion experiment started and time was monitored.

Once the gels had been diffusing for a specific time the various regions of the cell were collected. Six different regions that were collected and sliced parallel to the gel-gel interface as described in the paper. Every region from the gel was placed in an 8 mL vial and dried under high vacuum to remove the solvent. *For those experiments using ^1H NMR analysis*, the samples were redissolved in 1 mL of deuterated toluene. Six different NMR tubes were obtained representing the 6 different regions of the cell for a given diffusion time. The various NMR spectra were integrated in terms of proton signals to determine the corresponding concentrations of the different components in each region. This allowed analysis of concentrations and hence diffusion profiles. *For those experiments using CD analysis*, the dried sample was accurately weighed and made up to a solution concentration of 5 mM in methylcyclohexane:dioxane (95:5) and then analysed by CD spectrometry. Using both of these methods, we estimate errors on calculated concentrations to be ± 0.25 mM.

3 Rheology of Gels

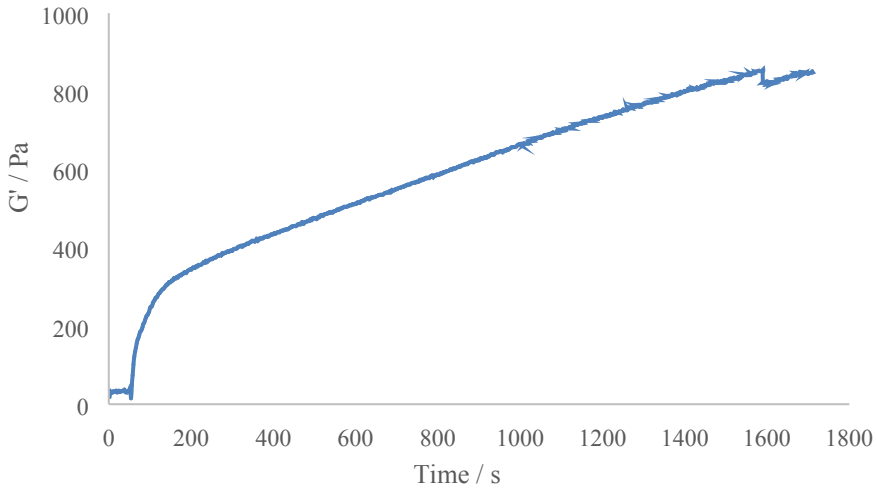

Fig. S1. Plot showing the progression of gelation as monotored by G' on mixing L-Lys-G2-CO_2H with hexylamine in toluene on the rheometer plate at 25ºC.

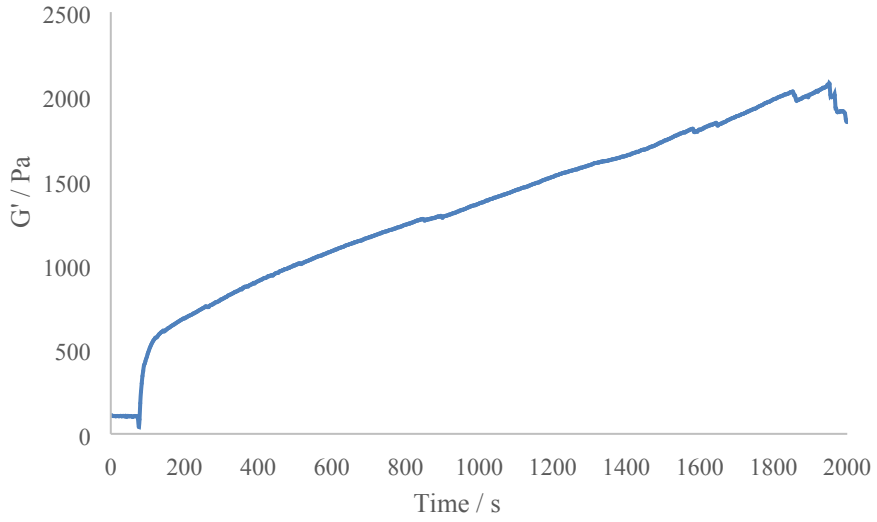

Fig. S2. Plot showing the progression of gelation as monotored by G' on mixing L-Lys-G2-CO_2H with 1-naphthylmethylamine in toluene on the rheometer plate at 25ºC.

3 Imaging of Gels

3.1 Atomic Force Microscopy Images

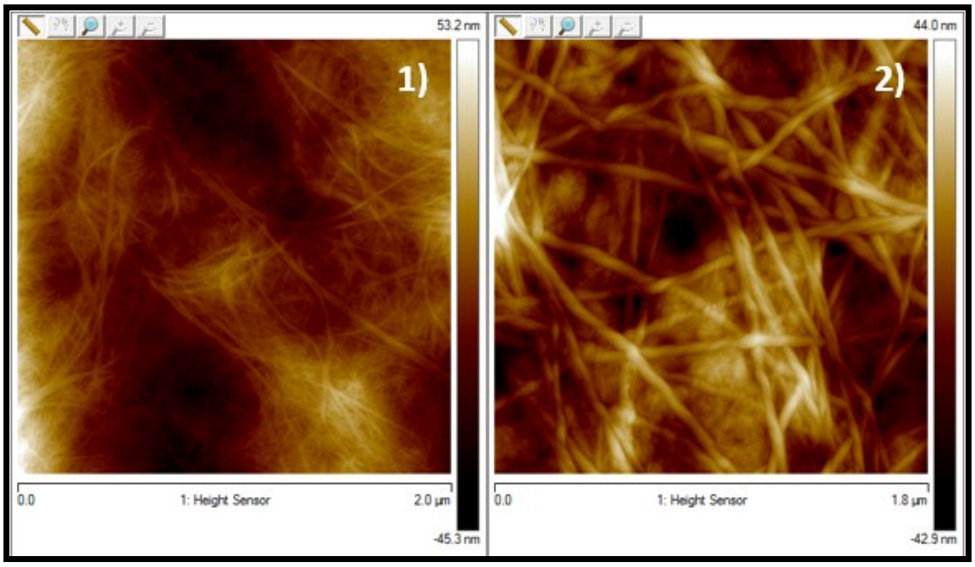

Figure S3. AFM images of L-Lys-NaphGel fibres (1) and L-Lys-HexGel nanofibres (2). Samples formed by simple mixing of the two-components in solution at room temperature followed by ambient drying.

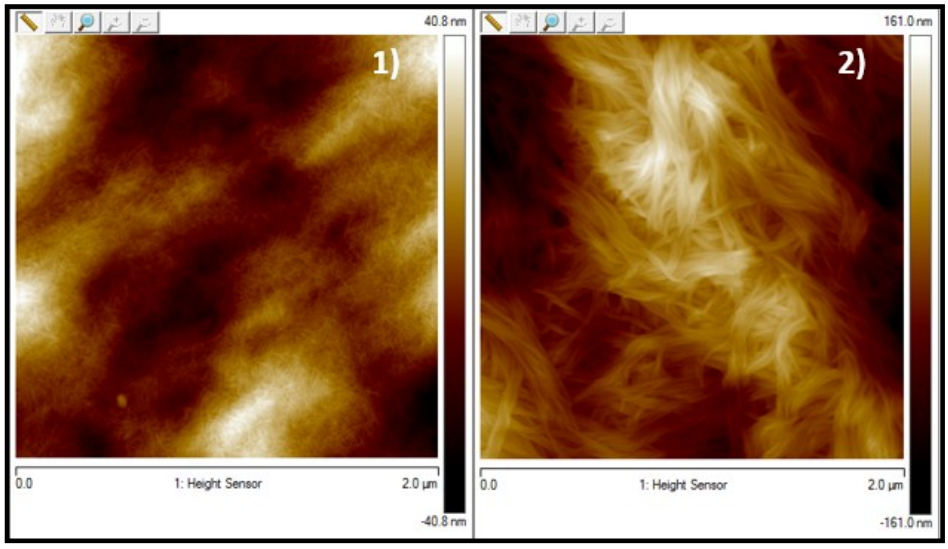

Figure S4. AFM images of L-Lys-NaphGel fibres (1) and L-Lys-HexGel nanofibres (2). Samples formed by mixing the two-components in solution at room temperature and application of a heat-cool cycle to anneal the gel, followed by ambient drying.

3.2 Transmission Electron Microscopy Images

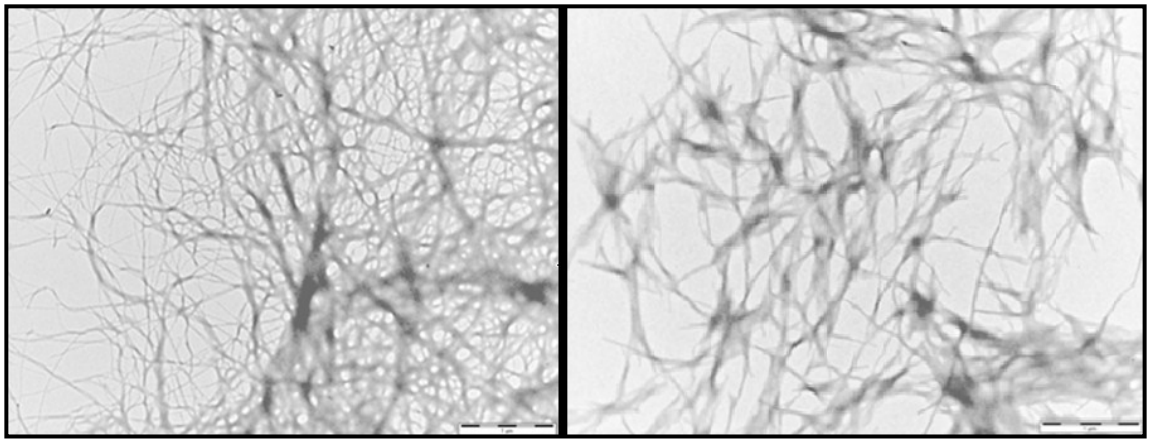

Figure S5. TEM images of L-Lys NaphGel (left) and L-Lys-HexGel (right) at 16,500 magnification (scale bar = 1 μm).

3.3 Scanninng Electron Microscopy Images

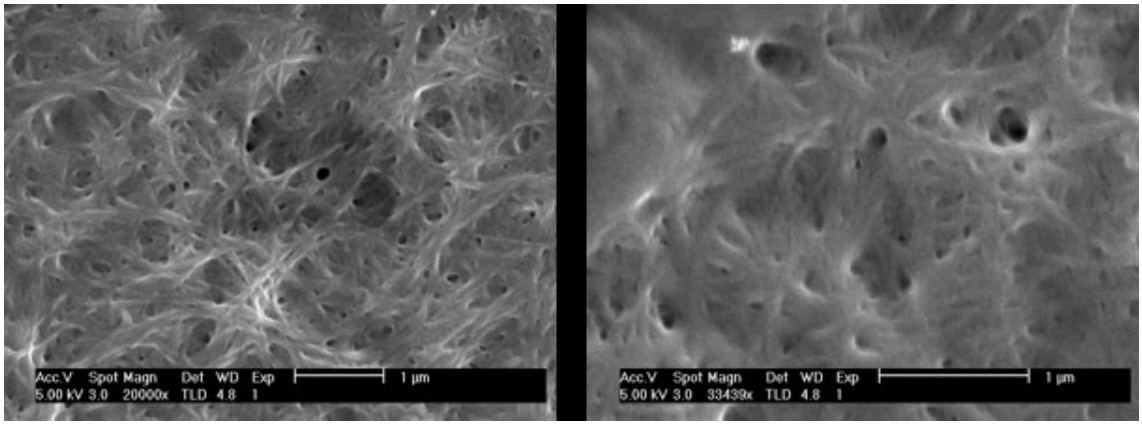

Figure S6. SEM images of L-Lys-HexGel (10 mM) dried under ambient conditions. Xerogels. Left 20.000 magnification, right 33.439 magnification (scale bars = 1 μm).

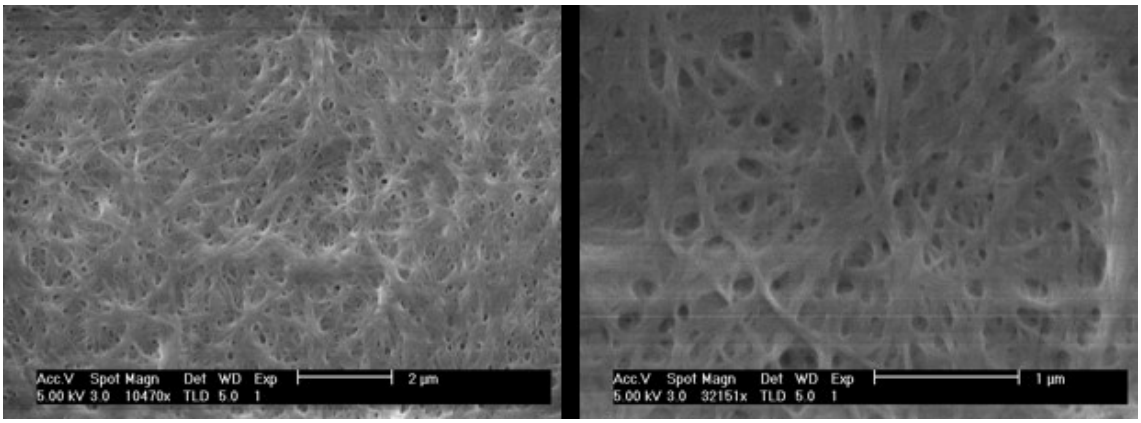

Figure S7. SEM images of L-Lys-NaphGel (10 mM) dried under ambient conditions. Xerogels. Left 20,000 magnification, right 33,439 magnification (scale bars = 2 µm (left) and 1 µm (right)).

4 VT ^{1}H NMR of Gels

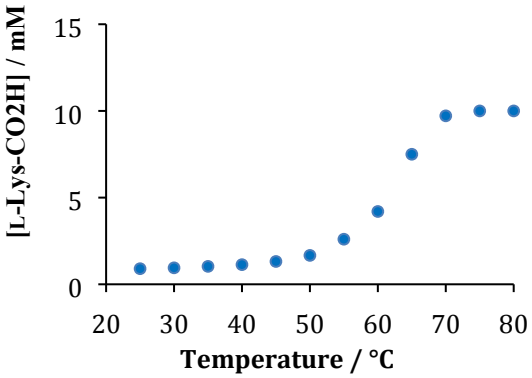

Figure S8. Concentration of L-Lys-G2-CO_2H (as determined by ^{1}H NMR spectroscopy) visible in gels formed with hexylamine as temperature increases in toluene-d_8. It is evident that some of the dendron can be observed at room temperature, and hence has mobility on the NMR timescale. The original data and methods appear in reference 2.

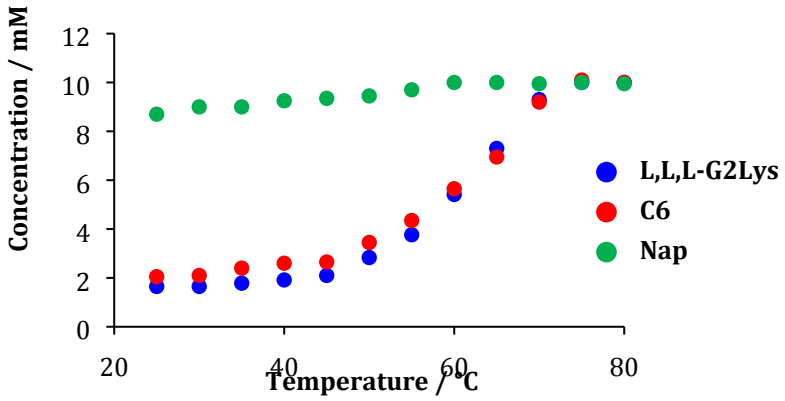

Figure S9. Concentration of components visible in ^{1}H NMR as temperature increases in a component selection gel experiment with L-Lys-G2-CO_2H (10 mM), hexylamine (C6, 10 mM) and 1-naphthylmethylamine (Nap, 10 mM) in toluene-d_8. It is evident that hexylamine complexes preferentially to the dendron over 1-naphthylmethylamine, as a result of its higher pKa value. The original data and methods appear in reference 2.

5 Construction of Diffusion Cell

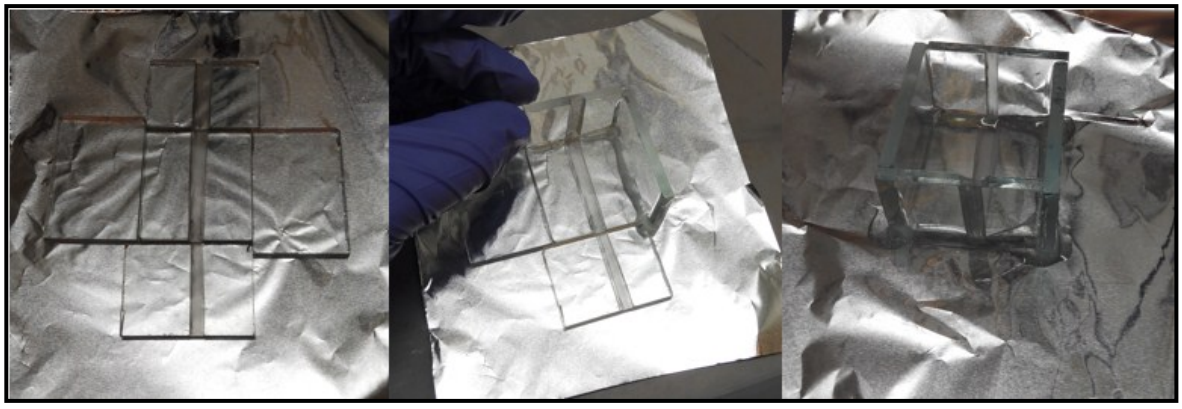

Figure S10. Assembly of glass diffusion cells from individual components.

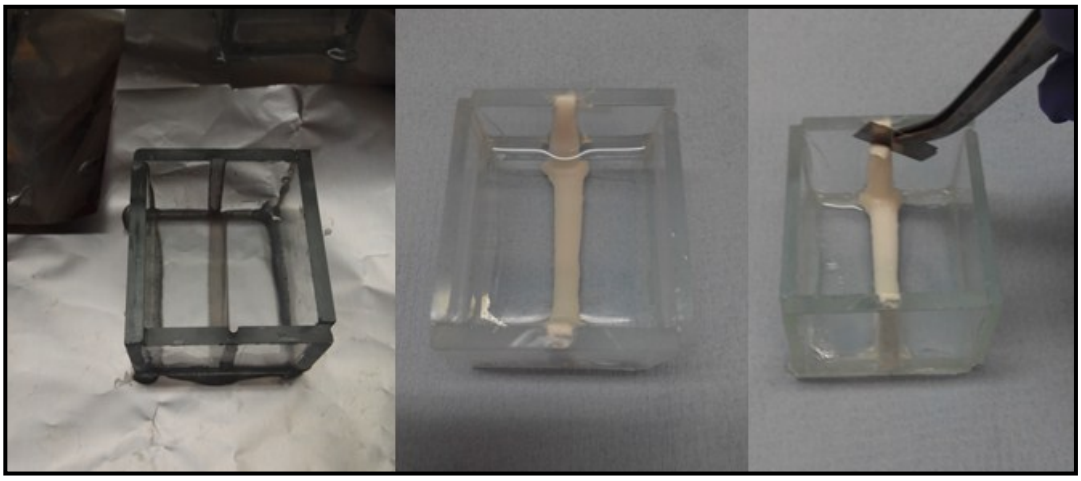

Figure S11. The process of joining the two sides of the diffusion cell using white silicone in order to seal one side from the other with an aluminium barrier. Once silicone is in contact with toluene it swells and there was therefore a need to remove the excess swollen white silicone with a very sharp blade to obtain a completely flat surface in the diffusion cell.

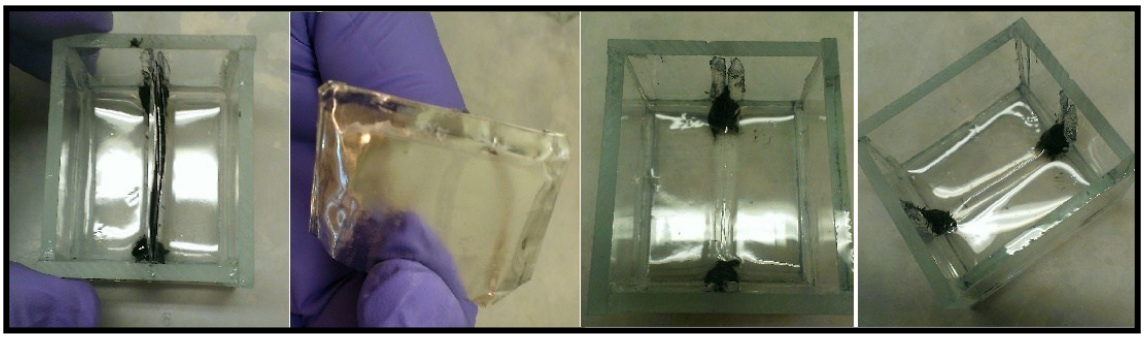

Figure S12. Placement of the gels in the cuvette and removal of the aluminium separator from the cell in order to start the diffusion experiment.

6 TEM Imaging After Diffusion Experiment

Imaging was performed after 48 h of diffusion between L-Lys-HexGel and L-Lys-NaphGel.

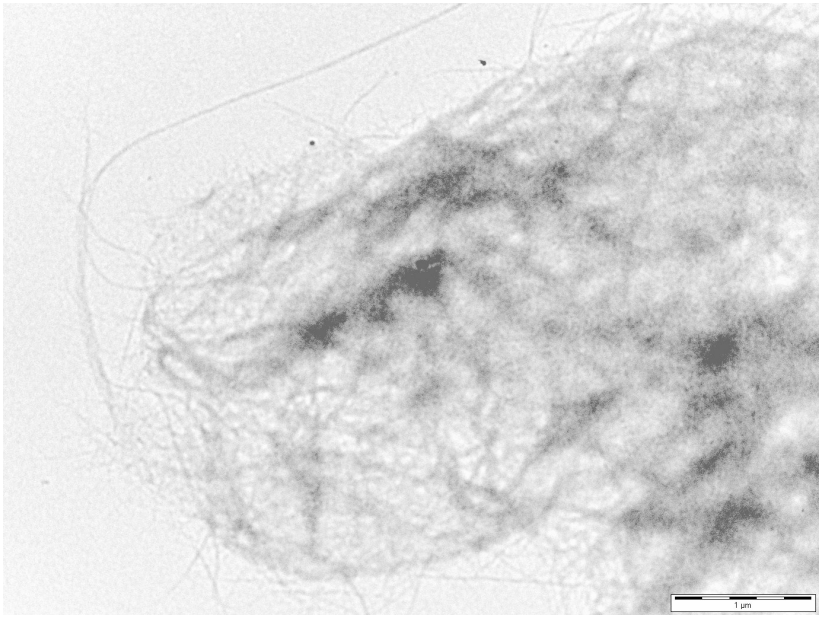

Figure S13. TEM image of gel sampled from region 1 of the diffusion cell 48 hours after the start of the diffusion experiment. The fibres appear typical morphologies of L-Lys-NaphGel.

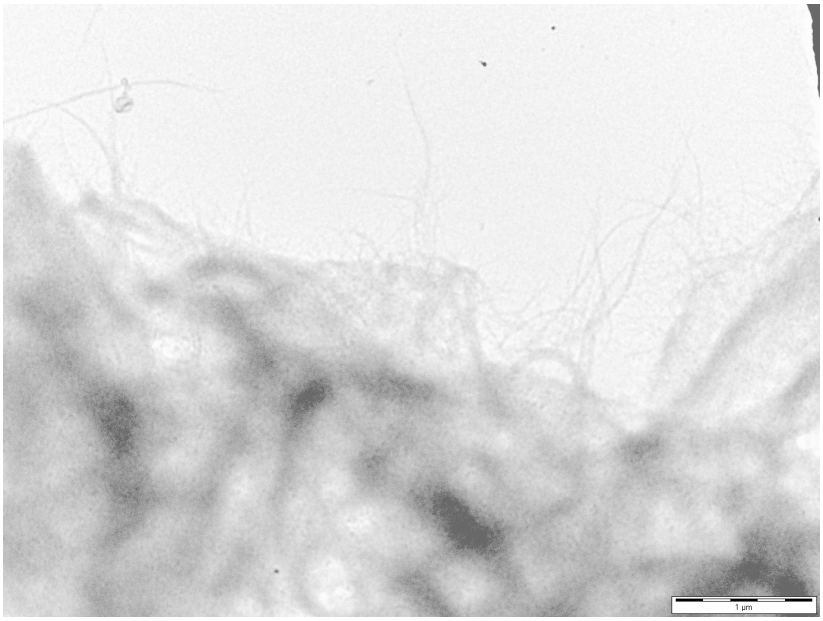

Figure S14. TEM image of gel sampled from region 2 of the diffusion cell 48 hours after the start of the diffusion experiment. The fibres appear typical morphologies of L-Lys-NaphGel.

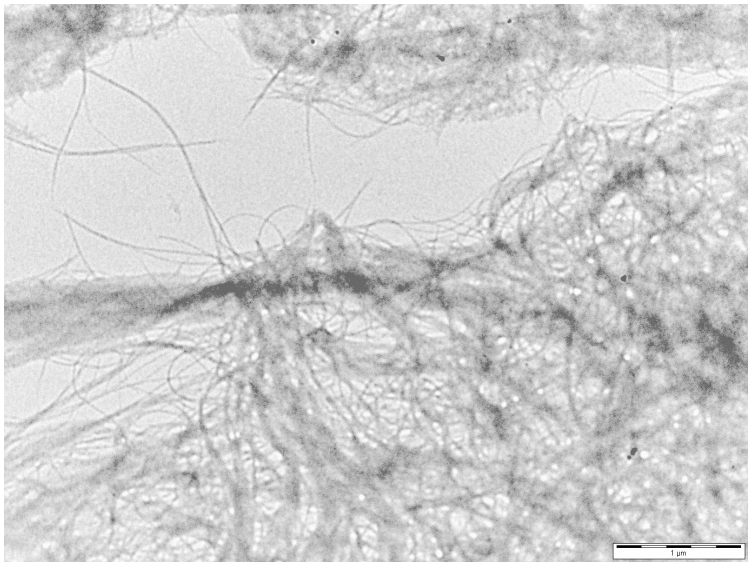

Figure S15. TEM image of gel sampled from region 3 of the diffusion cell 48 hours after the start of the diffusion experiment. The fibres appear typical morphologies of L-Lys-NaphGel, although they appear better defined than samples from regions 1 and 2, which may represent some influence of diffused hexylamine in this region.

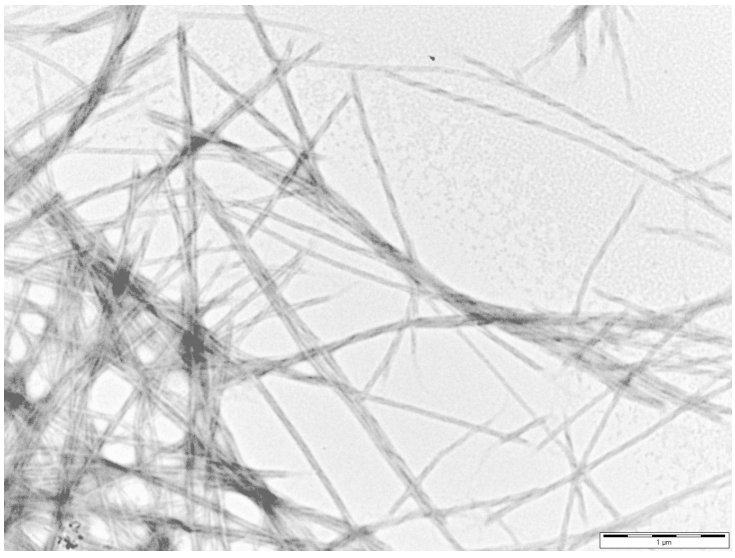

Figure S16. TEM image of gel sampled from region 4 of the diffusion cell 48 hours after the start of the diffusion experiment. The fibres appear typical morphologies of L-Lys-HexGel,

although they appear more helical than samples from regions 5 and 6, which may represent some influence of diffused 1-naphthylmethylamine in this region.

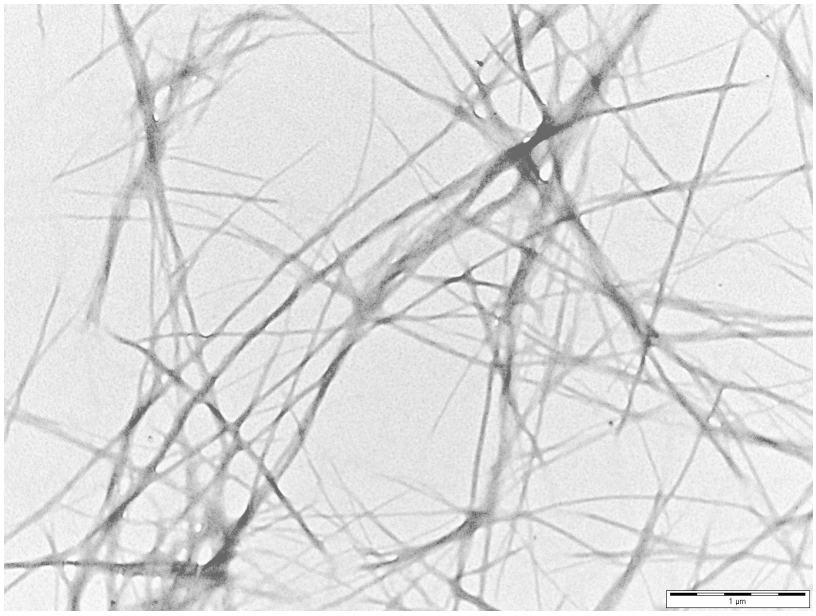

Figure S17. TEM image of gel sampled from region 5 of the diffusion cell 48 hours after the start of the diffusion experiment. The fibres appear typical morphologies of L-Lys-HexGel.

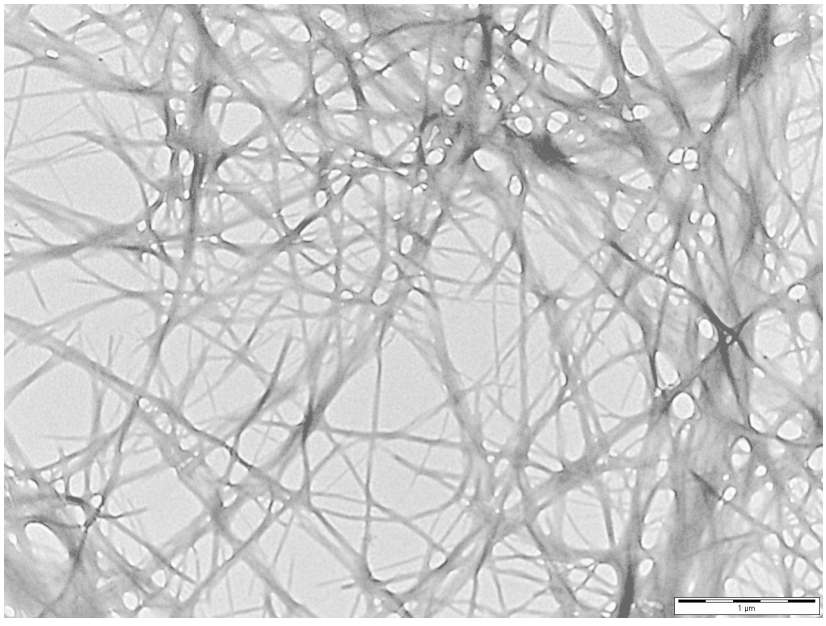

Figure S18. TEM image of gel sampled from region 6 of the diffusion cell 48 hours after the start of the diffusion experiment. The fibres appear typical morphologies of L-Lys-HexGel.

7 Data from Diffusion Cell Experiments

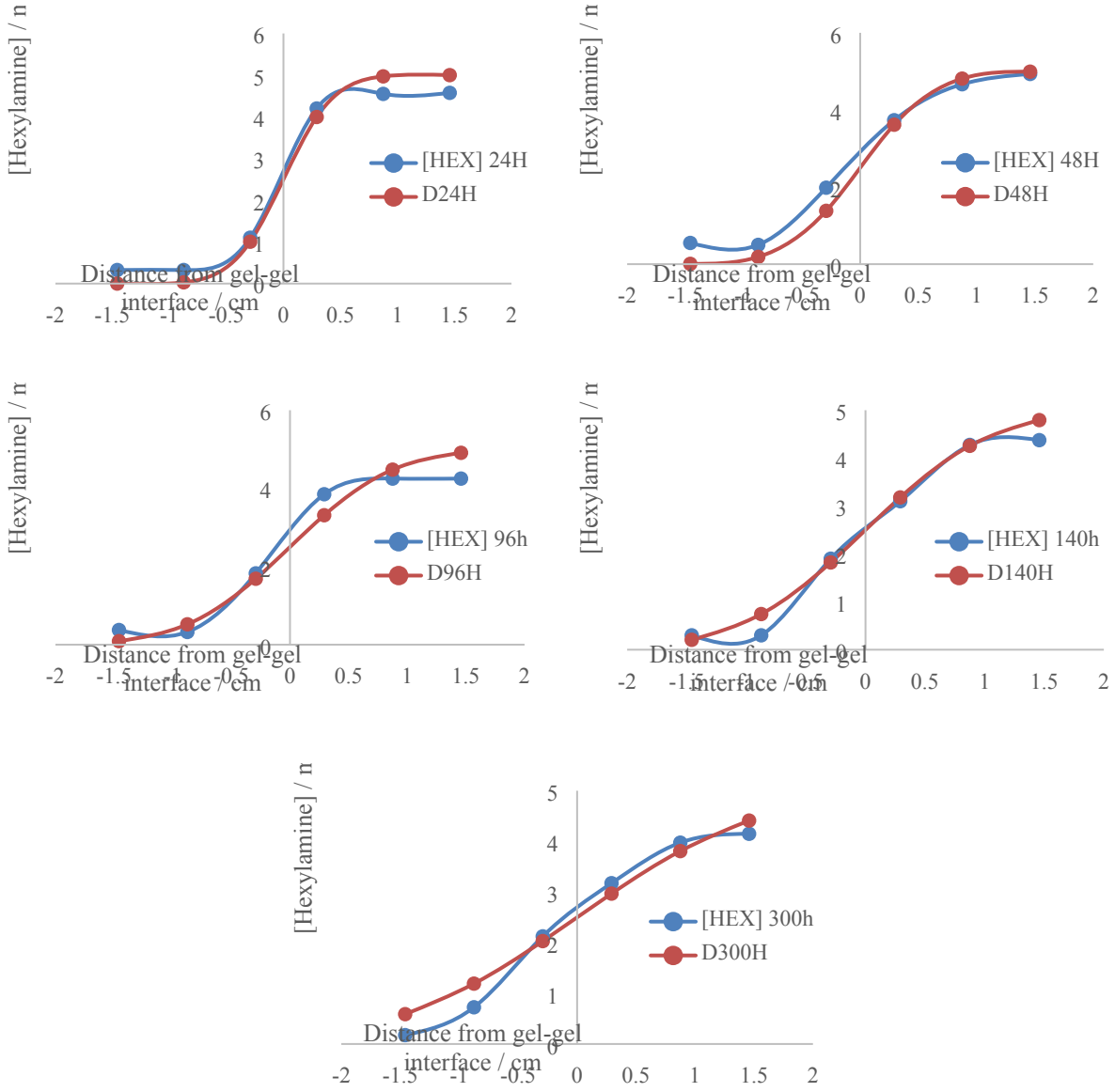

Figure S19. Concentration profiles for hexylamine from the diffusion experiment at 25°C at 24 h, 48 h, 96 h, 140 h and 300 h respectively. Experimental data are shown in blue. Fitting to the simple model based on Fick's law is shown in red. All fits have been refined simultaneously using a least squares method to obtain the best overall global fit of data, and

hence estimate the average diffusion coefficient, D. Lines between data points are a guide to the eye.

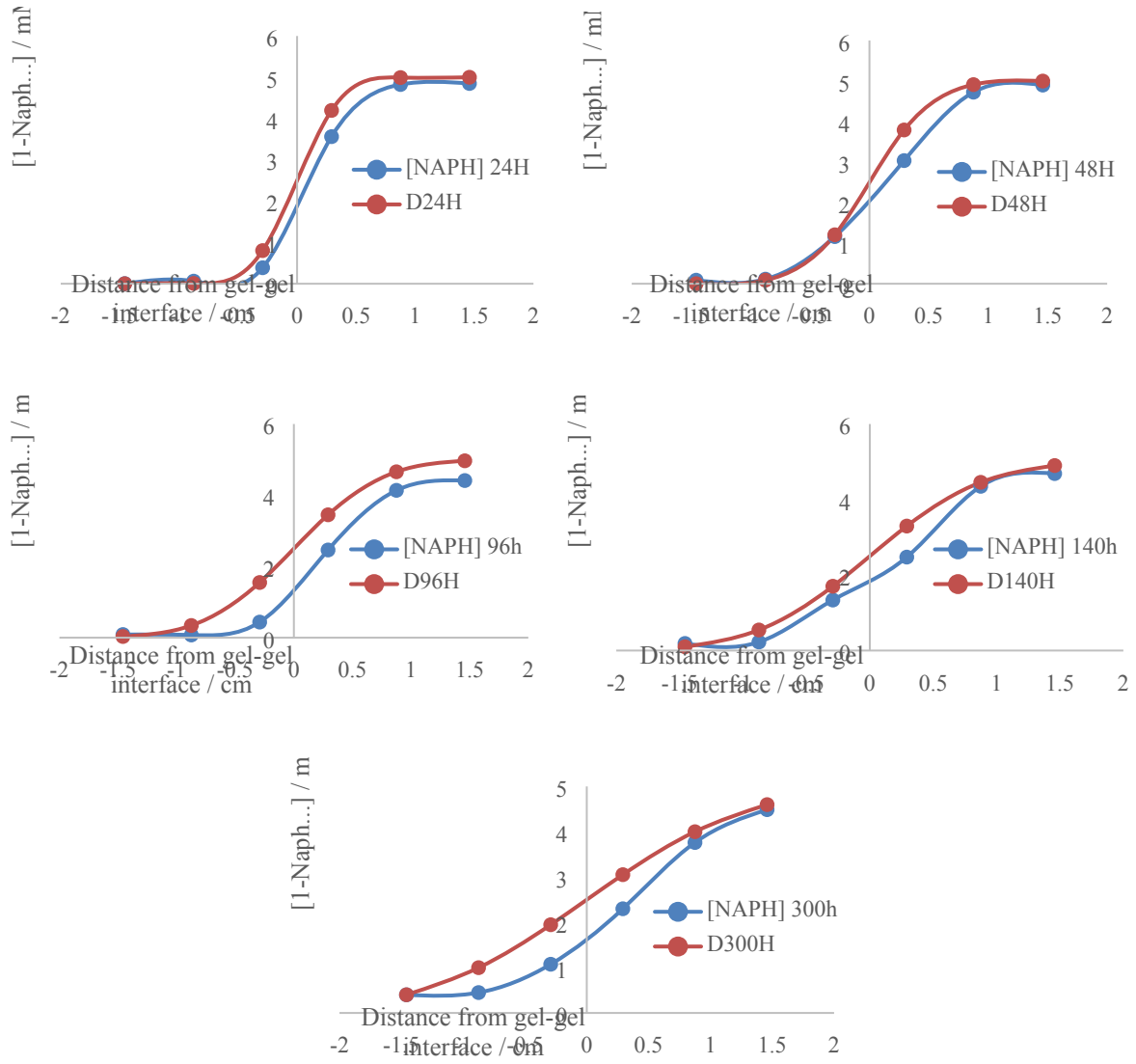

Figure S20. Concentration profiles for 1-methylnaphthylamine from the diffusion experiment at 25°C at 24 h, 48 h, 96 h, 140 h and 300 h respectively. Experimental data are shown in blue. Fitting to the simple model based on Fick's law is shown in orange. All fits have been refined simultaneously using a least squares method to obtain the best overall global fit of data, and hence estimate the average diffusion coefficient, D. Lines between data points are a guide to the eye.

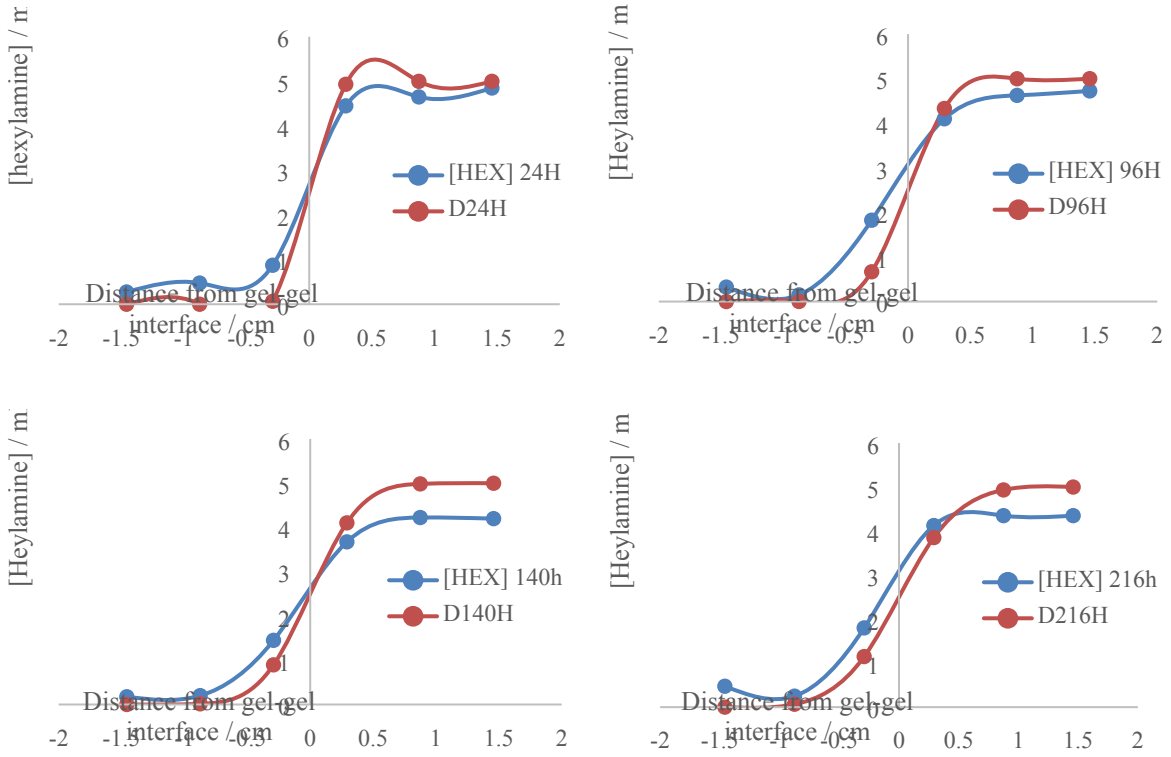

Figure S21. Concentration profiles for hexylamine from the diffusion experiment at 5°C at 24 h, 96 h, 140 h and 216 h respectively. Experimental data are shown in blue. Fitting to the simple model based on Fick's law is shown in red. All fits have been refined simultaneously using a least squares method to obtain the best overall global fit of data, and hence estimate the average diffusion coefficient, D. Lines between data points are a guide to the eye.

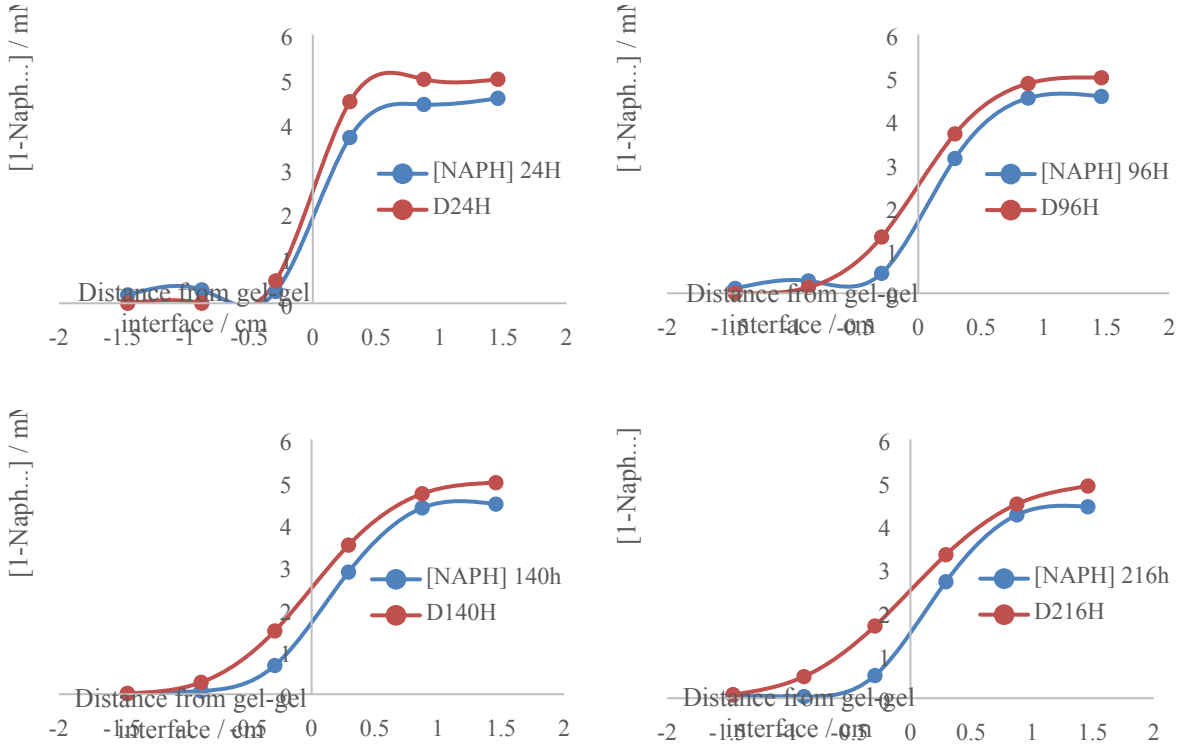

Figure S22. Concentration profiles for 1-naphthylmethylamine from the diffusion experiment at 5°C at 24 h, 96 h, 144 h and 216 h respectively. Experimental data are shown in blue. Fitting to the simple model based on Fick's law is shown in red. All fits have been refined simultaneously using a least squares method to obtain the best overall global fit of data, and hence estimate the average diffusion coefficient, D. Lines between data points are a guide to the eye.

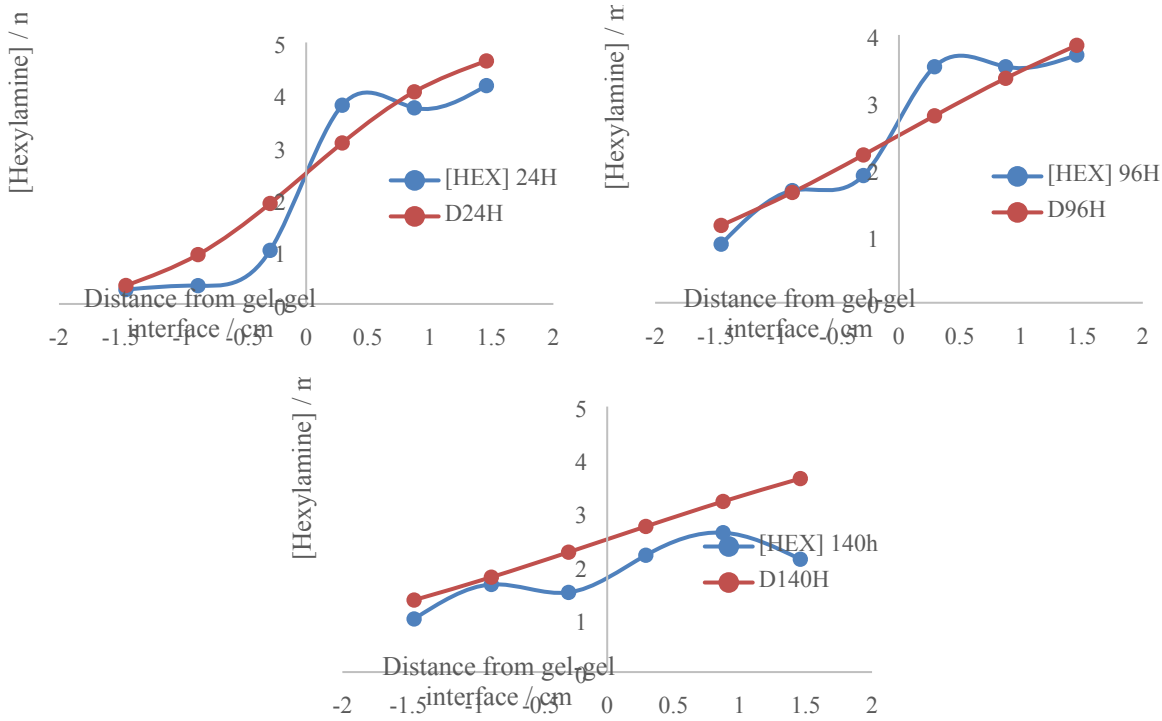

Figure S23. Concentration profiles for hexylamine from the diffusion experiment at 45°C at 24 h, 96 h and 140 h respectively. Experimental data are shown in blue. Fitting to the simple model based on Fick's law is shown in red. All fits have been refined simultaneously using a least squares method to obtain the best overall global fit of data, and hence estimate the average diffusion coefficient, D. Lines between data points are a guide to the eye.

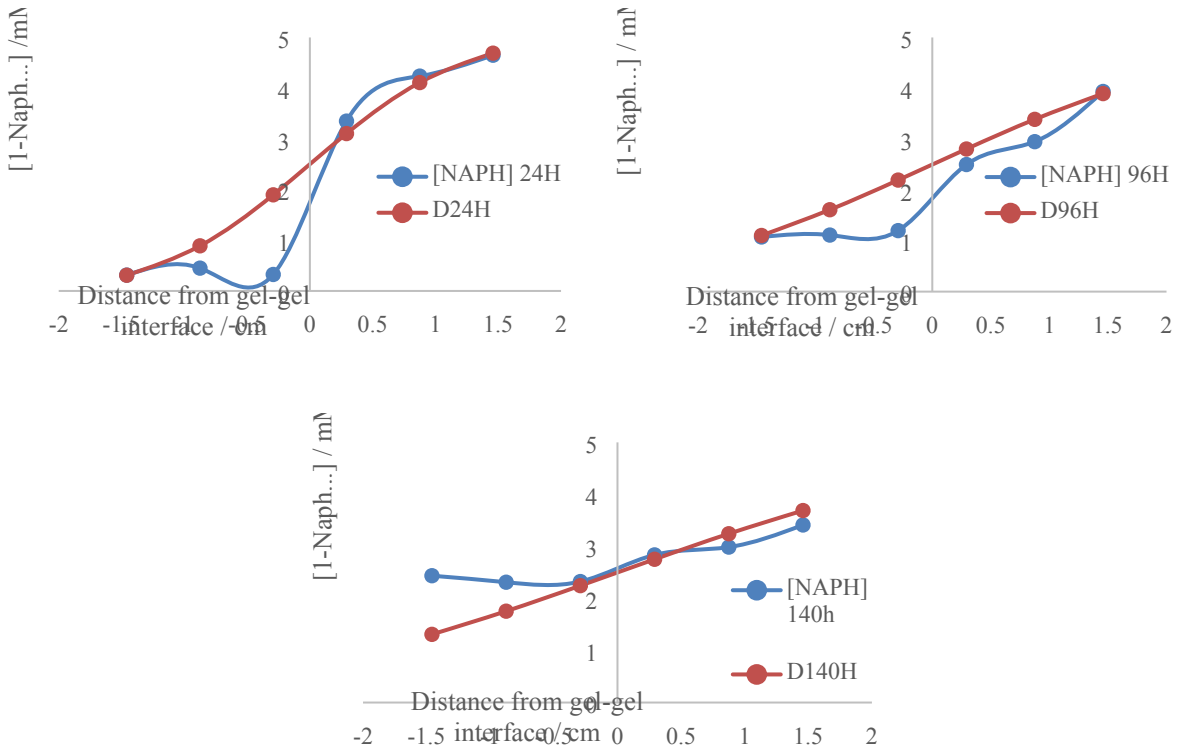

Figure S24. Concentration profiles for 1-naphthylmethylamine from the diffusion experiment at 45°C at 24 h, 96 h and 140 h respectively. Experimental data are shown in blue. Fitting to the simple model based on Fick's law is shown in red. All fits have been refined simultaneously using a least squares method to obtain the best overall global fit of data, and hence estimate the average diffusion coefficient, D. Lines between data points are a guide to the eye.

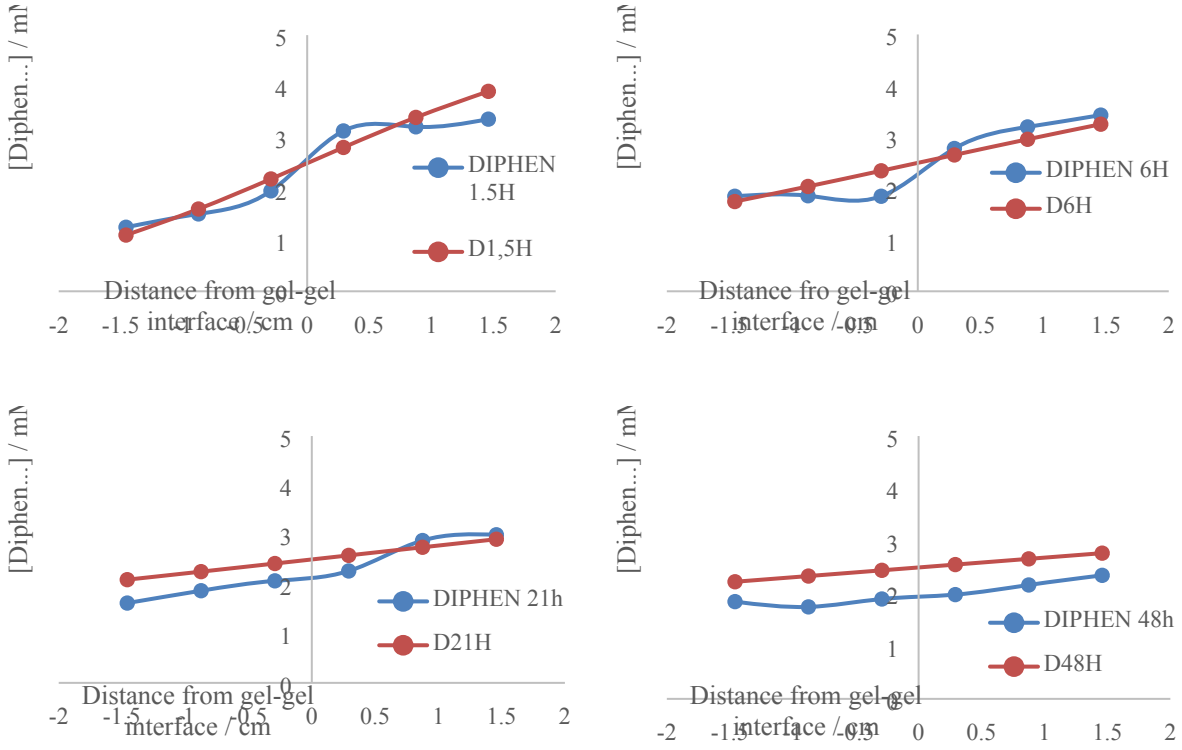

Figure S25. Concentration profiles for diphenylmethane from the diffusion experiment at 25°C at 1.5 h, 6 h, 21 h and 48 h respectively. Experimental data are shown in blue. Fitting to the simple model based on Fick's law is shown in red. All fits have been refined simultaneously using a least squares method to obtain the best overall global fit of data, and hence estimate the average diffusion coefficient, D. Lines between data points are a guide to the eye.

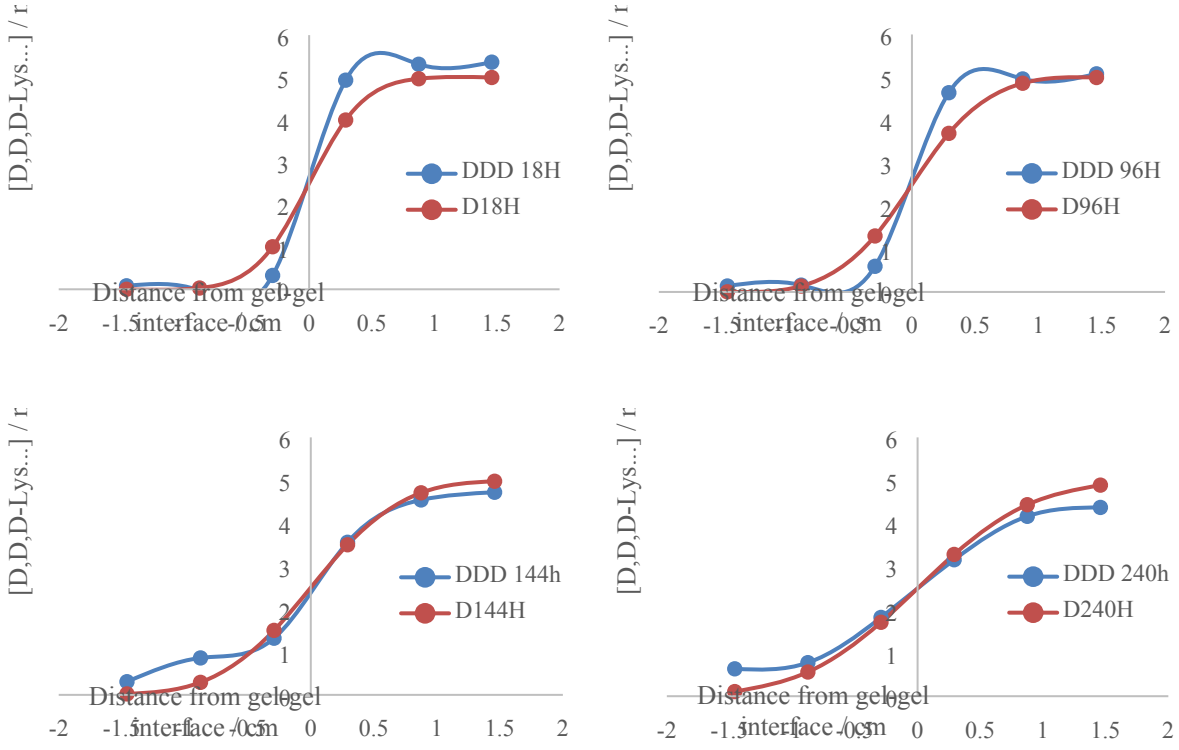

Figure S26. Concentration profiles for D-Lys-G2-CO_2H from the diffusion experiment at 25°C at 18 h, 96 h, 144 h and 240 h respectively. Experimental data are shown in blue. Fitting to the simple model based on Fick's law is shown in red. All fits have been refined simultaneously using a least squares method to obtain the best overall global fit of data, and hence estimate the average diffusion coefficient, D. Lines between data points are a guide to the eye.

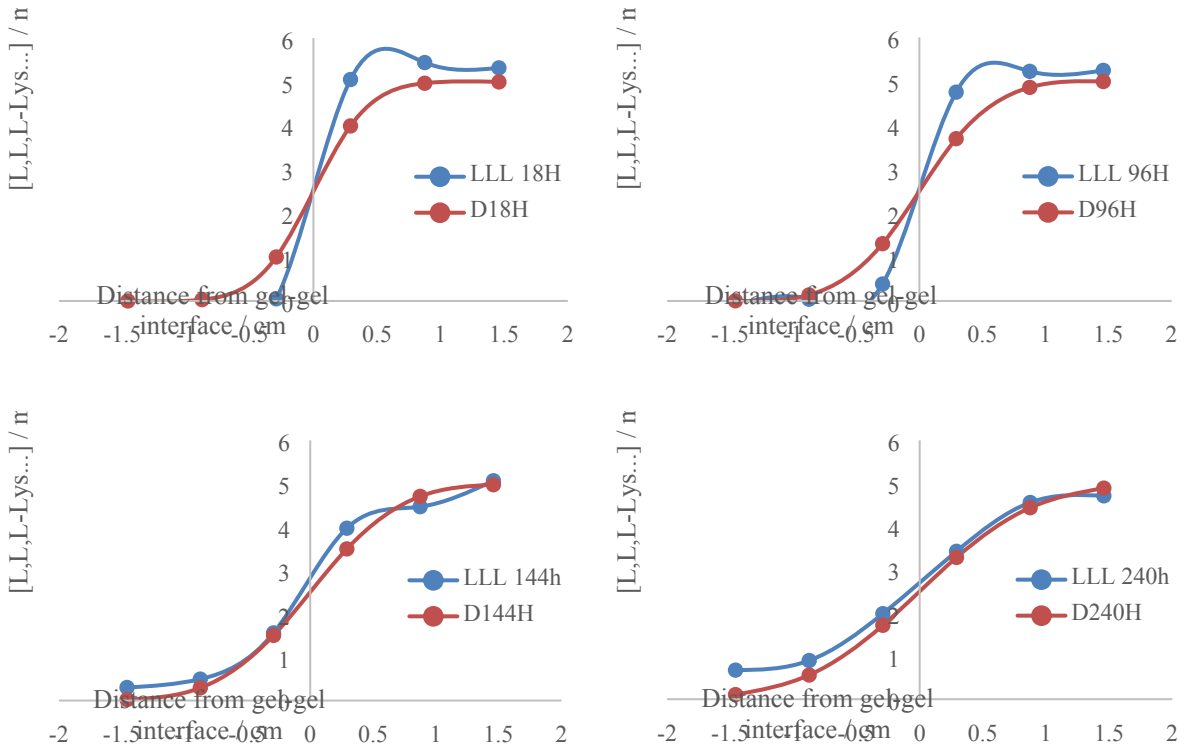

Figure S27. Concentration profiles for L-Lys-G2-CO_2H from the diffusion experiment at 25°C at 18 h, 96 h, 144 h and 240 h respectively. Experimental data are shown in blue. Fitting to the simple model based on Fick's law is shown in red. All fits have been refined simultaneously using a least squares method to obtain the best overall global fit of data, and hence estimate the average diffusion coefficient, D. Lines between data points are a guide to the eye.

7 CD Spectra from Diffusion Cell Expriments

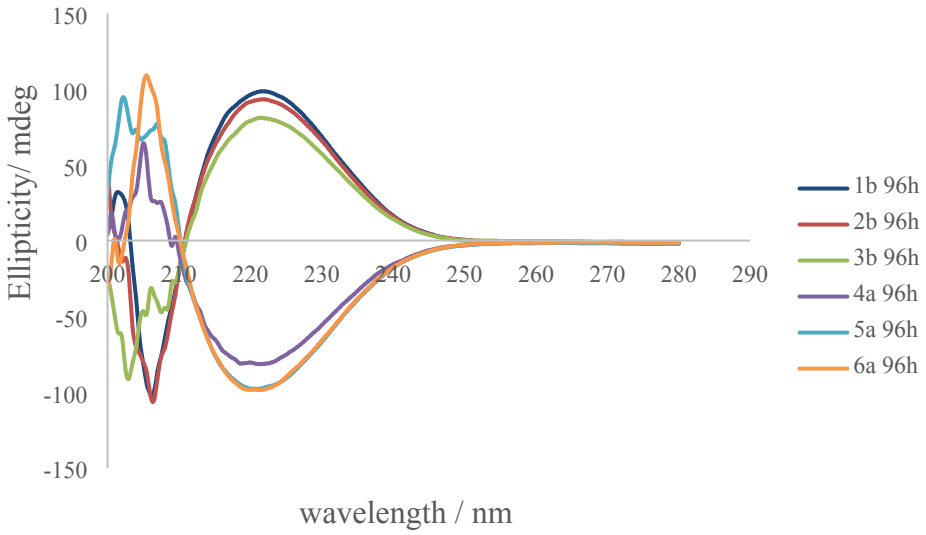

Figure S28. CD spectra for the diffusion cell experiment using L-Lys-HexGel and D-Lys-HexGel after diffusion has progressed for 96h. Spectra 1-6 correspond to samples taken from regions 1-6 of the diffusion cell respectively.

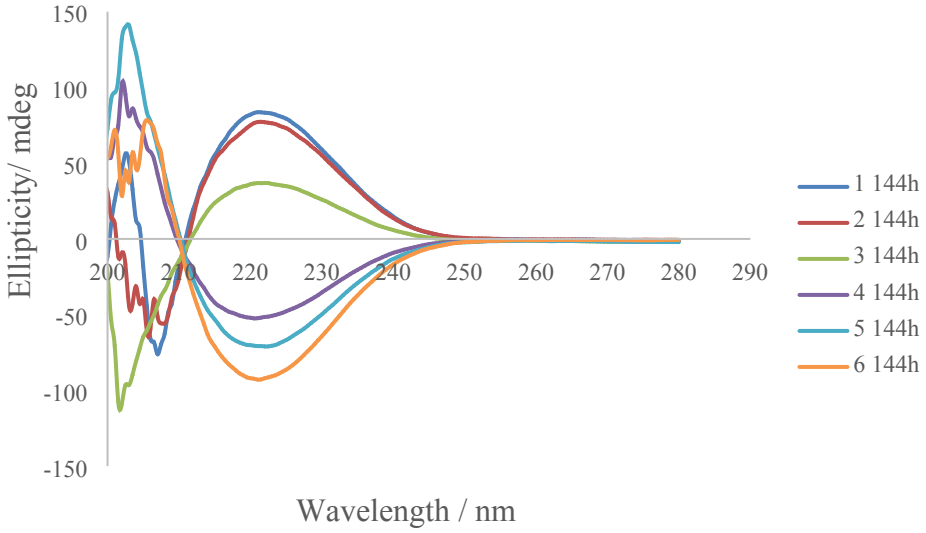

Figure S29. CD spectra for the diffusion cell experiment using L-Lys-HexGel and D-Lys-HexGel after diffusion has progressed for 144 h. Spectra 1-6 correspond to samples taken from regions 1-6 of the diffusion cell respectively.

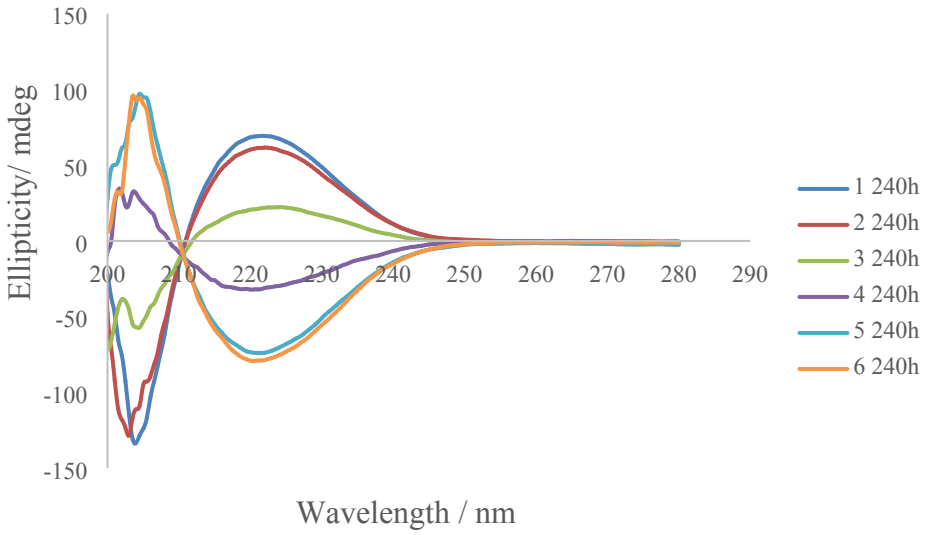

Figure S30. CD spectra for the diffusion cell experiment using L-Lys-HexGel and D-Lys-HexGel after diffusion has progressed for 240 h. Spectra 1-6 correspond to samples taken from regions 1-6 of the diffusion cell respectively.

8 References

1. (*a*) K. S. Partridge G. M. Dykes, D. K. Smith and P. T. McGrail, *Chem. Commun.* 2001, 319-320. (*b*) G. M. Dykes, L. J. Brierley, D. K. Smith, P. T. McGrail and G. J. Seeley, *Chem. Eur. J.* 2001, **7**, 4730-4739. (*c*) A. R. Hirst, D. K. Smith, M. C. Feiters and H. P. M. Geurts, *Chem. Eur. J.*, 2004, **10**, 5901-5910. (*d*) W. Edwards and D. K. Smith, *J. Am. Chem. Soc.* 2014, **136**, 1116-1124.
2. W. Edwards and D. K. Smith, *J. Am. Chem. Soc.* 2013, **135**, 5911-5920.